Dimensional control of turbine blades via RSM-based process parameter optimization in investment casting

Sheng-jie Ren[1, 2, 3], Rui-yuan Zhang[1,2], Sheng Meng[2], Hang-yu Li[1], Wen-jing Wang[1], Zhong-min Xiao[3], and *Kun Bu[1,2]

1. Key Laboratory of High Performance Manufacturing for Aero Engine, Ministry of Industry and Information Technology, Northwestern Polytechnical University, Xi'an 710072, China ;
2. Engineering Research Center of Advanced Manufacturing Technology for Aero Engine, Ministry of Education, Northwestern Polytechnical University, Xi'an 710072, China ;
3. School of Mechanical and Aerospace Engineering, Nanyang Technological University, Singapore 639798, Singapore.

*Corresponding: Kun Bu, female, Ph. D., Professor. Her research interests focus primarily on turbine blade investment casting and numerical simulation of the forming process.

E-mail: pukun89@nwpu.edu.cn

Abstract: To address the dimensional deviation challenges in the investment casting of hollow turbine blades, this study proposes a multi-parameter collaborative optimization and deformation response prediction method based on response surface methodology. Taking pouring temperature, shell temperature, and withdrawal rate as key variables, deformation response data are obtained through numerical simulation, and a second-order model incorporating linear, interaction, and quadratic terms is established to characterize the nonlinear coupling effects of process parameters on dimensional deformation. The results indicate that withdrawal rate is the dominant factor influencing deformation, while shell temperature exhibits a pronounced "U"-shaped nonlinear trend. Significant interactions between process parameters are also observed. The constructed model demonstrates high predictive accuracy, with R2 of 0.978 and an RMSE of 0.0026 mm, and exhibits strong generalization capability, enabling the identification of optimal parameter combinations even beyond the simulated dataset. Compared with conventional orthogonal design methods, the optimized process reduced the predicted maximum deformation from 0.2047 mm to 0.1905 mm, achieving an improvement of approximately 6.95%. This work provides a theoretical foundation and practical strategy for dimensional accuracy control and multi-parameter process optimization in the manufacturing of complex thin-walled castings.

Keywords: Response surface method; Turbine blade; Process parameter optimization; Investment casting

1 Introduction

Investment casting is a critical manufacturing process for high-performance hollow turbine blades, in which process parameters exert a decisive influence on both the forming quality and dimensional accuracy of the castings [1, 2]. With the increasing structural complexity and performance requirements of turbine blades, significant coupling effects have emerged among key process variables such as withdrawal rate, pouring temperature, and preheating temperature during casting [3-5]. These interactions are recognized as major contributors to deformation and dimensional deviation in cast components [6-8]. Therefore, systematically identifying the dominant process parameters and their interactions has become a core challenge in improving the dimensional precision and consistency of turbine blades.

In recent years, with the rapid advancement of numerical simulation technologies, extensive research has been conducted on solidification-based numerical analysis and process optimization in investment casting [4, 9-11]. These efforts have significantly contributed to shortening development cycles, reducing experimental costs, and improving product quality. Hoda Dini et al. [12] employed a single-factor control approach to investigate the effects of process parameters on residual stress and dimensional variation in castings. Ma et al. [13] studied the influence of thermal gradients and withdrawal rates on defect formation during Bridgman directional solidification. Miller et al. [14] determined optimal process conditions by analyzing the position and morphology of the solid–liquid interface. Galantucci et al. [15] used the finite element method to simulate temperature field evolution during directional solidification and examined the impact of filling temperature, withdrawal rate, and furnace geometry on the thermal gradient. Tian et al. [16] conducted orthogonal experiments to optimize process parameters, resulting in a 21.8% reduction in flange deformation. K. Niranjan et al. [17] designed a multi-factor, multi-level experimental scheme and validated the derived model, achieving a prediction accuracy exceeding 95% for the mechanical properties of the material.

Although previous studies have made notable progress in process parameter optimization, most remain limited to single-factor analysis, making it difficult to fully capture the interactions among variables and their synergistic effects on dimensional deformation [18-20]. In contrast, response surface methodology (RSM) offers the ability to construct high-order regression models incorporating interaction terms, while maintaining strong modeling accuracy and optimization capability. These features make it suitable for addressing the complexity and coupling investment casting process optimization.

Based on this, the present study employs RSM to model and optimize the multi-parameter combinations involved in the investment casting of turbine blades. By investigating the dimensional deformation behavior under various process conditions, this work aims to provide both theoretical support and methodological guidance for the precision manufacturing of complex cast components.

2 Materials and methods

2.1 Experimental procedure

The directional solidification of directionally solidified or single-crystal turbine blades is a complex process involving the coupling of multiple physical fields and influencing factors. From alloy melting to solidification, the entire process is conducted under vacuum conditions.

As illustrated in Fig. 1, the directional solidification system and its corresponding numerical modeling process for single-crystal turbine blades are presented. Fig. 1(a) shows the structural schematic of the casting, including the gating system, ceramic core, blade body, starter block, and grain selector, which together define the functional layout along the vertical axis. Fig. 1(b) illustrates the numerical simulation model, incorporating the mold geometry and the heating–cooling zone configuration designed to reproduce the thermal gradient environment. Fig. 1(c) displays the experimental directional solidification apparatus, in which the mold is gradually withdrawn from the heating furnace into the cooling chamber to achieve controlled unidirectional solidification. The entire process was carried out in a vacuum induction furnace, sequentially involving alloy melting, mold filling, directional solidification, and constraint removal.

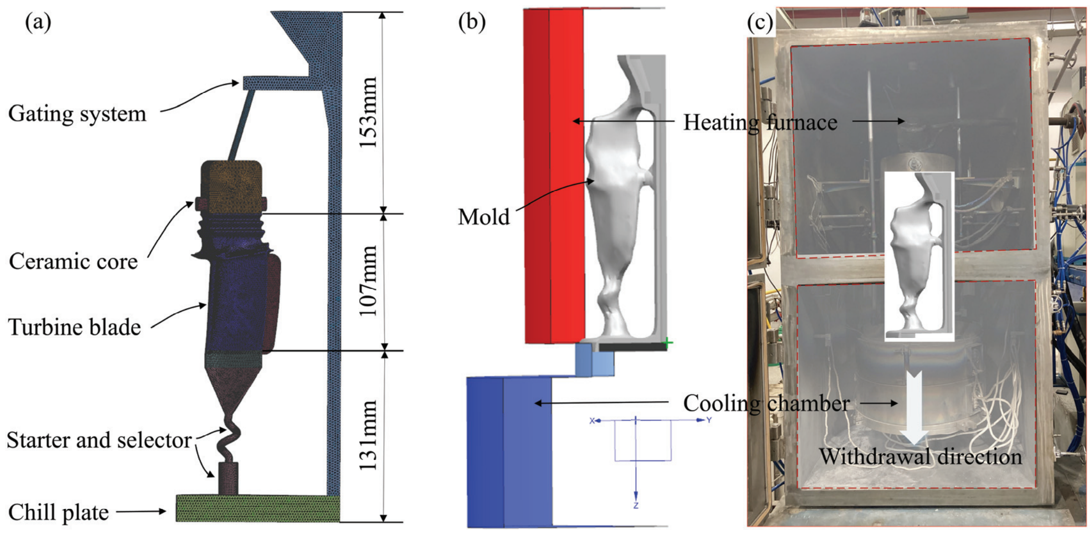

Fig. 1: Experimentation and modeling of turbine blade directional solidification

In the experiment, 5 kg of DD6 single-crystal superalloy was melted under a vacuum pressure of $3\times10^{□3}$□ Pa and subsequently poured from the top into the mold shell, which had a thickness of 7.5 mm. After a short holding period to achieve thermal equilibrium, the mold was withdrawn downward at a specified rate, enabling its gradual transition from the high-temperature zone to the low-temperature zone. This movement established a longitudinal temperature gradient along the blade axis, promoting the formation of a directionally solidified structure.

Table 1 Nominal chemical composition of single-crystal superalloy DD6

Element	C	Cr	Co	W	Mo	Al	Nb	Ta	Re	Hf	Ni
wt%	0.2	4.3	9	8	2	5.7	1.2	7.2	2	0.1	Bal

During the early stage of solidification, heat transfer occurred primarily via thermal conduction in the downward direction. However, as the solid–liquid interface progressed upward, the thermal conductivity decreased and the dominant heat dissipation mechanism gradually shifted from conduction to radiation [21-24]. Further experimental details are illustrated in Fig. 1(a).

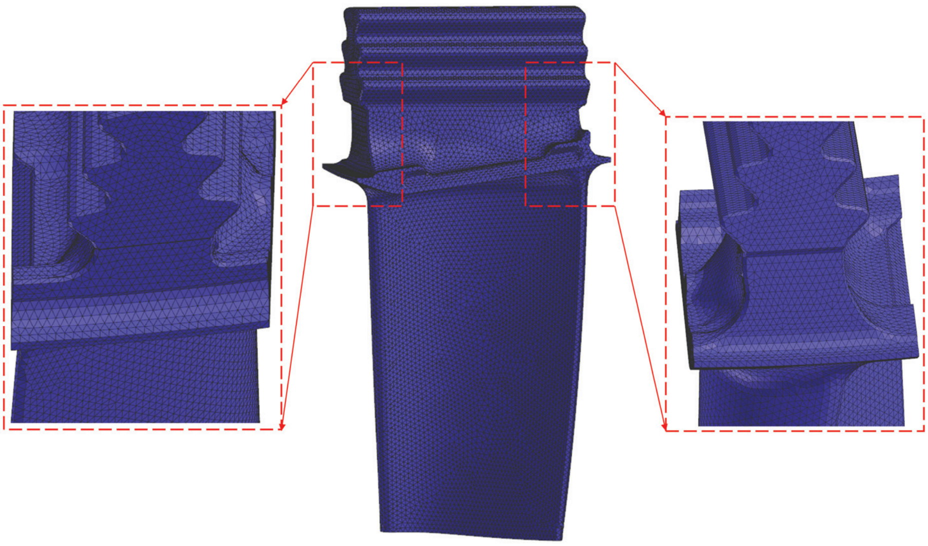

Fig. 2: Surface mesh of the gating system

To improve computational accuracy and efficiency, as shown in Fig. 2, a non-uniform finite element mesh was employed in the model, with element sizes ranging from 0.5 to 15 mm. Approximately 1.07 million elements were generated in total, with local mesh refinement applied to critical regions such as the blade root junction and interface transition zones.

2.2 Boundary conditions

To ensure the accuracy of the thermal property data for the alloy, this study calibrated and fitted key thermal parameters of the DD6 nickel-based superalloy—such as thermal conductivity and density—based on experimental measurements and simulations using JMatPro and ProCAST software, such as thermal conductivity, density, enthalpy and fraction solid. As shown in Fig. 3, the obtained material properties serve as essential input for the subsequent coupled thermal–mechanical simulations of the temperature and stress fields.

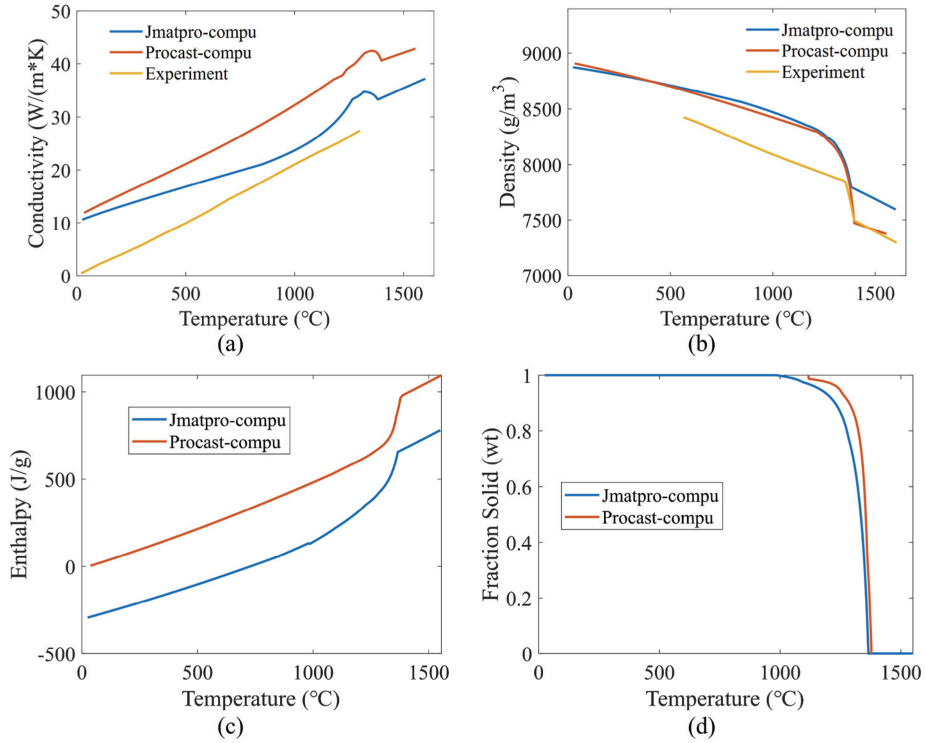

Fig. 3: Partial thermophysical parameters of the nickel-based superalloy DD6: (a) conductivity; (b) density; (c) enthalpy and (d) fraction solid

The heat transfer between the furnace and the mold shell was primarily considered to occur via thermal radiation, with the radiation direction oriented toward the interior of the furnace. The radiation emissivity was set to 0.7, as referenced in [4, 25].

Under these assumptions the equation for heat transfer in castings can be simplified to [26, 27].

$$\rho c \frac{\partial T}{\partial t} = \lambda \left(\frac{\partial^2 T}{\partial x^2} + \frac{\partial^2 T}{\partial y^2} + \frac{\partial^2 T}{\partial z^2} \right) + Q \qquad (1)$$

where ρ is the density, kg/m^3; c is the specific heat, J/(kg · K); T is temperature, K; x, y, and z represent coordinates; λ is the heat conductivity, W/(m·K); Q is the radiation heat between the casting surface and its environment, W/m^3.

The temperature of the liquid metal is uniformly distributed at the initial time of solidification.

$$T(x, y, z, t)\big|_{t=0} = T_0 \qquad (2)$$

where T_0 is the initial superalloy temperature.

According to the Stefan-Boltzmann's law, the radiation from the inner surface of the furnace and the outer surface of the mold shell yield

$$q = \varepsilon\sigma(T_s^4 - T_a^4) \qquad (3)$$

where q is the heat flux density, J/m^2; ε is the emissivity, value in [0, 1]; σ is the Stefan–Boltzmann constant; T_s and T_a are surface and ambient temperature, respectively.

2.3 Response surface method

RSM is a statistical analysis approach widely used in experimental design and process parameter optimization, particularly suitable for addressing complex problems involving nonlinear behavior and multi-factor interactions. By systematically varying experimental conditions, RSM enables the construction of functional relationships between input variables and response variables. The response is typically fitted using a second-order polynomial regression model, which is expressed as follows [28-30]

$$y = \beta_o + \sum_{i=1}^{k} \beta_i x_i + \sum_{i=1}^{k} \sum_{j=1}^{k} \beta_{ij} x_i x_j + \sum_{i=1}^{k} \beta_{ii} x_i^2 \qquad (4)$$

where y represents the predicted response, x is the independent variables, and β corresponds to the regression coefficients.

Fig. 4 presents the geometric layout of experimental points constructed using the Box–Behnken design (BBD), aimed at exploring the influence of three key process parameters on dimensional accuracy during the investment casting of turbine blades. As one of the most used experimental designs in RSM, BBD is particularly suitable for optimization involving two to five factors [31-34].

In the 3D parameter space, blue solid spheres denote the BBD design points, positioned at the midpoints of the edges of the cubic design space, while the red central point represents the repeated center run used for estimating experimental error and model curvature. This structured sampling strategy ensures balanced evaluation of parameter interactions while avoiding extreme corner points, thereby improving both the safety and statistical robustness of the experimental plan.

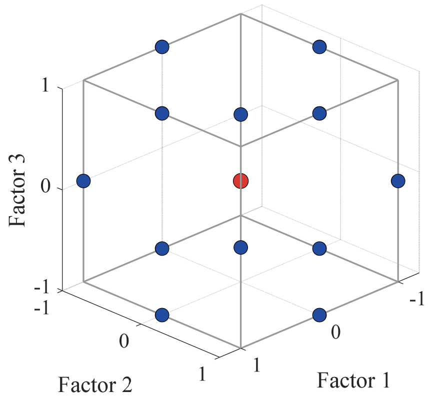

Fig. 4: Spatial distribution of BBD points in a three-factor parameter space for investment casting optimization.

This design requires the specification of three levels for each factor: the high level (+1), the low level (–1), and the center point (0). Notably, all experiments are confined within the defined design space and do not involve extreme or extrapolated conditions beyond the specified range.

Table 2. Experimental Variables and Levels

Process parameters	Symbol	Levels		
		-1	0	1
Pouring temperature (℃)	A	1520	1550	1580
Shell temperature (℃)	B	1450	1475	1500
Withdrawal rate (mm/min)	C	2	2.5	3

Pouring temperature T_p(℃), shell temperature T_s(℃), and withdrawal rate v(mm/min) were selected as the process variables, while the blade deformation was taken as the target response. As shown in Table 2, each of the three process parameters was set at three levels, coded as –1, 0, and +1, corresponding to the low, center, and high levels, respectively.

Table 3. Some Experimental Matrices for RSM Designs Based on Three Level Variables

No.	Influencing factors			Response
	A	B	C	Deformation (mm)
1	1520	1450	2.5	0.2170
2	1520	1500	2.5	0.2204
3	1520	1475	2	0.2039
4	1520	1475	3	0.2232
5	1550	1450	2	0.2047
6	1550	1500	2	0.2043
7	1550	1450	3	0.2277
8	1550	1500	3	0.2261
9	1550	1475	2.5	0.2056
10	1550	1475	2.5	0.2057
11	1550	1475	2.5	0.2053
12	1550	1475	2.5	0.2052
13	1550	1475	2.5	0.2051
14	1580	1450	2.5	0.2103
15	1580	1500	2.5	0.2150
16	1580	1475	2	0.2021
17	1580	1475	3	0.2131

The experimental scheme and the corresponding response values are presented in Table 3. Based on the three selected process parameters, a total of 17 experimental runs were generated. The resulting deformation responses ranged from 0.18 mm to 0.23 mm. A nonlinear mathematical model was subsequently developed based on the BBD framework to describe the response surface.

3 Results and discussion

3.1 Directional solidification physical field analysis

The evolution of the temperature field provides a fundamental basis for analyzing the stress and displacement fields. By examining the temperature distributions at various time steps, the thermal evolution during the solidification process can be clearly captured, enabling the assessment of solidification mode, solidification sequence, and internal thermal gradients of the casting.

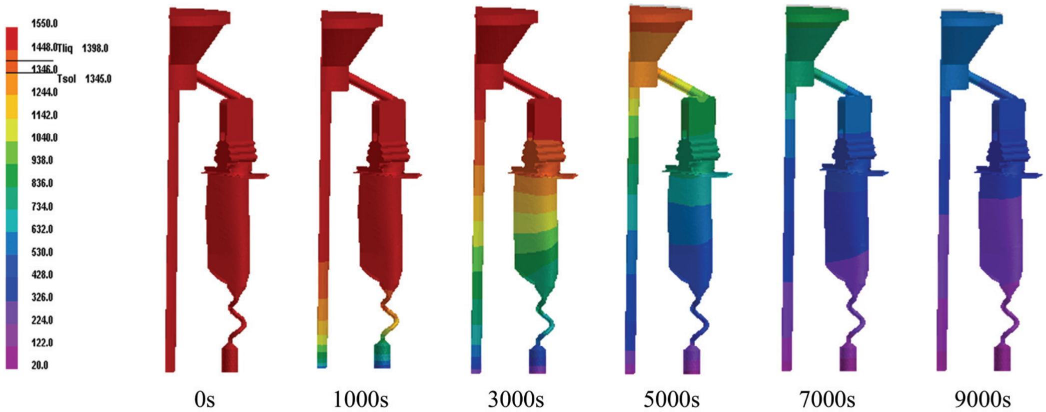

Fig. 5: Temperature field distribution during directional solidification of castings

As shown in Fig. 5, the temperature contour maps of the blade at the initial moment, 1000 s, 3000 s, 5000 s, 7000 s, and 9000 s illustrate the temperature evolution during the investment casting process. The results reveal a distinct vertical temperature gradient, with nearly horizontal isothermal lines, indicating that heat flow is predominantly conducted along the axial direction. This thermal condition facilitates the preferential vertical growth of the single crystal, which is consistent with the theoretical principles of directional solidification for single-crystal blades.

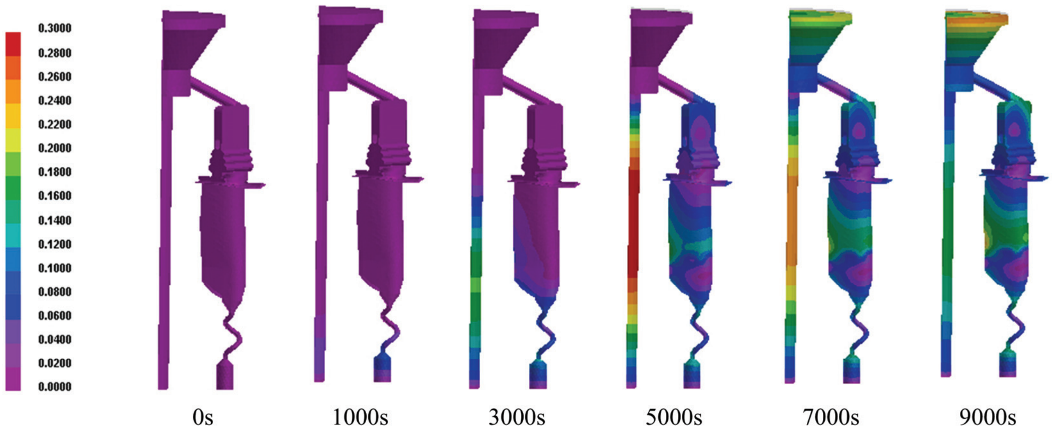

Fig. 6: Displacement field distribution during directional solidification of castings

Dimensional deviation is a critical issue in the investment casting of turbine blades. Minimizing deformation and ensuring high surface accuracy are essential objectives for improving casting quality. As illustrated in Fig. 6, the displacement contour maps at the initial moment, 1000 s, 3000 s, 5000 s, 7000 s, and 9000 s display the evolution of the displacement field throughout the casting process. These distributions enable a clear and intuitive observation of the deformation magnitude and trends in various regions of the casting, including the platform and trailing edge, thereby providing valuable insights into the overall deformation behavior during the entire investment casting process.

3.2 Influence of a single process parameter on casting dimensions

To further investigate the influence of key process parameters on the dimensional deformation response of the castings and to identify the optimal parameter combination for improving dimensional accuracy, this study employed a modeling and optimization approach based on RSM. Pouring temperature, shell temperature, and withdrawal rate were selected as the primary process variables.

To analyze the effect of each individual parameter while holding the other two at their center levels, response surface slice plots were generated. These plots illustrate how the target function—deformation magnitude—varies with changes in a single parameter under controlled conditions. The results are presented in Fig. 7.

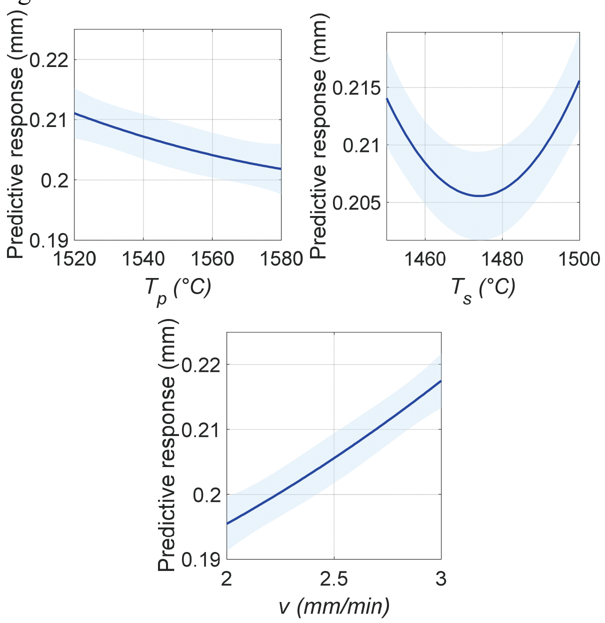

Fig. 7: Effect of three process parameters on predicted response.

The influence of pouring temperature on deformation was relatively minor, exhibiting a slight decreasing trend overall, indicating low sensitivity of this parameter to dimensional variation. In contrast, shell temperature showed a pronounced nonlinear effect on deformation, with a near "U"-shaped response curve. This suggests the existence of an optimal temperature range, where both excessively high and low values may lead to increased deformation. Withdrawal rate was identified as the most influential factor, with deformation increasing significantly as the rate increased, implying that a lower withdrawal rate is preferable for minimizing dimensional deviation.

Furthermore, the distribution of the confidence intervals indicates that the model yields higher predictive accuracy near the center of the design space. However, increased uncertainty is observed at the boundaries, likely due to a lower density of experimental data in those regions.

3.3 RSM-based process optimization results

The response values, representing the dimensional deviations of the castings under different process parameter combinations, were obtained through numerical simulation or experiments. These responses were modeled as functions of coded variables using a second-order response surface model incorporating linear, quadratic, and interaction terms. The resulting model was employed to characterize the individual effects of each process parameter on casting deformation, as well as the interactions among them.

$$\begin{aligned} Y = {} & 0.20557 - 0.00463A + 0.00077B + 0.01102C \\ & + 0.00033AB + 0.00117AC - 0.00032BC \\ & + 0.00088A^2 + 0.00926B^2 + 0.00091C^2 \end{aligned} \tag{5}$$

In the model, variables A, B, and C represent the normalized values of pouring temperature, shell temperature, and withdrawal rate, respectively, with each ranging from –1 to +1. The linear relationships between the actual physical parameters and the coded variables are detailed in Table 2. This model facilitates the analysis of main effects, interaction effects, and nonlinear behaviors of the process parameters, providing a theoretical foundation for subsequent optimization.

The root mean square error (RMSE) and the coefficient of determination (R^2) were used to evaluate the accuracy of the response surface model. The specific formula is as follows:

$$RMSE = \sqrt{\frac{1}{n}\sum_{i=1}^{n}\left(y_i - \hat{y}_i\right)^2} \tag{6}$$

$$R^2 = 1 - \left(\frac{\sum_{i=1}^{n}\left(y_i - \hat{y}_i\right)^2}{\sum_{i=1}^{n}\left(\bar{y}_i - \hat{y}_i\right)^2}\right) \tag{7}$$

where y_i and $\hat{y}_i$ are the true value and predicted value of the casting samples, respectively, and $\bar{y}_i$ denotes the sample mean. The smaller the RMSE value, the closer the R^2 is to 1, i.e., the smaller the difference between the model's predicted value and the true value, the better the model's performance.

The statistical characteristics of the model indicate strong fitting accuracy and predictive capability: the coefficient of determination was R^2=0.978, the analysis of variance yielded a significant F-value of 24.2 with a p-value of 0.00132, and the RMSE was 0.0026 mm.

As shown in Fig. 8, 3D response surfaces and 2D contour plots were generated based on the RSM model to illustrate the interaction effects of process parameters on flange deformation. In each case, the third parameter was fixed at its central level.

Fig. 8(a) and (b) show a curved response surface, indicating strong interaction between T_s and T_p. At low T_p, deformation is more sensitive to T_s; at high T_p, the surface flattens, suggesting greater stability. The contour plot reveals an elliptical optimal region, with lower deformation in the medium-to-high temperature range.

Fig. 8(c) and (d) show that deformation increases monotonically with *v*, confirming it as a dominant factor. Higher T_p mitigates this trend. Dense contour lines at high v indicate steep response gradients and highlight the need to tightly control v for dimensional accuracy.

Fig. 8(e) and (f) show a distinct valley shape, indicating an optimal withdrawal rate range within a certain T_s interval. Deformation decreases as T_s drops, but rises again at low T_s, likely due to reduced shell stiffness and increased thermal stress. Symmetric contour lines further confirm the existence of an optimal region.

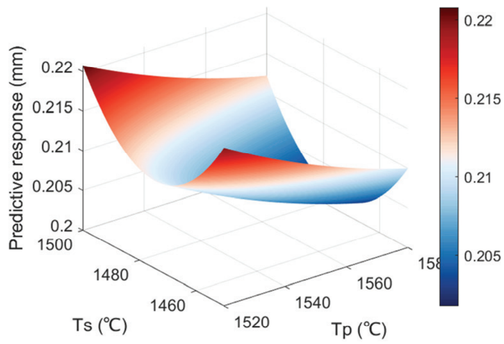

(a)

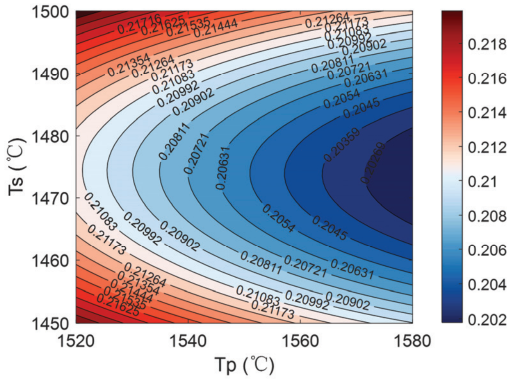

(b)

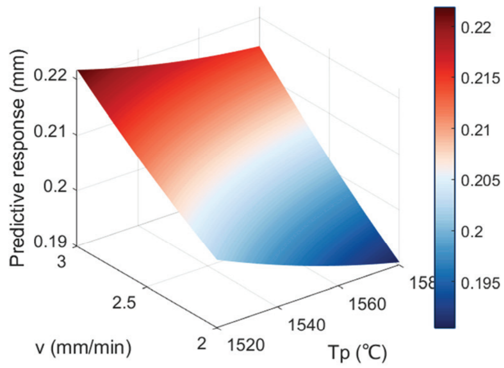

(c)

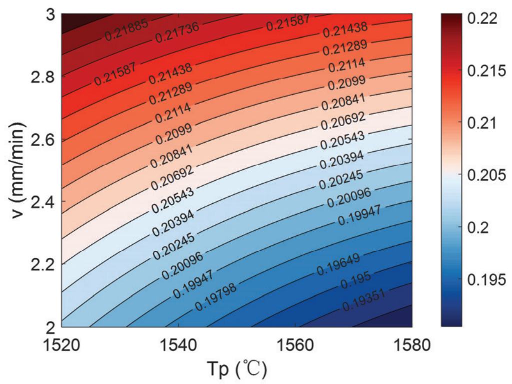

(d)

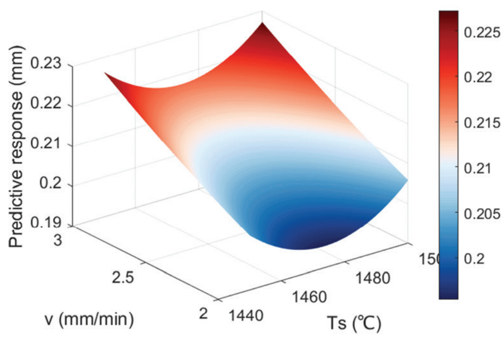

(e)

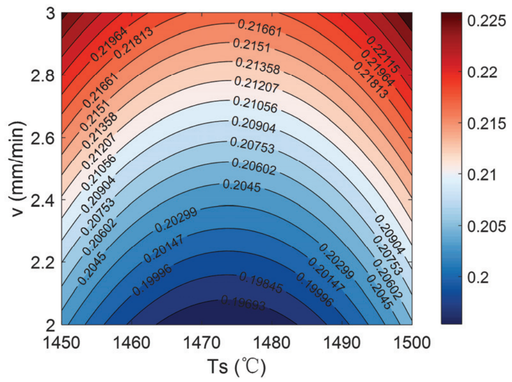

(f)

Fig. 8: Interaction effects of process parameters on the deformation response of turbine blades: (a) pouring temperature vs. shell temperature; (c) pouring temperature vs. withdrawal rate; (e) shell temperature vs. withdrawal rate — 3D response surface plots. (b), (d), and (f) are the corresponding 2D contour plots for (a), (c), and (e), respectively.

Based on the established model, an objective function was defined to minimize the response value. Constrained optimization was performed within the coded variable range of [–1, 1] to identify the optimal parameter combination corresponding to the minimum deformation. The optimal solution was then mapped back to actual physical values using linear interpolation, as summarized in Table 4.

Table 4. Comparison of optimization results between orthogonal and RSM for dimensional deviation minimization of turbine blades

Method	Tp	TS	V	Response (mm)
Orthogonal	1550	1450	2	0.2047
RSM	1580	1473	2	0.1905

As shown in Table 4, the RSM-derived optimal parameters—pouring temperature 1580 °C and shell temperature 1473 °C—effectively reduced the deformation from 0.2047 mm to 0.1905 mm under a fixed withdrawal rate, achieving a reduction of approximately 6.95%.

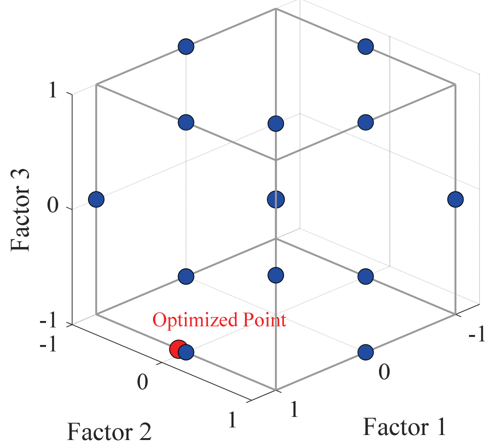

Fig. 9: Location of the optimized solution in the normalized BBD space.

The red point in Fig. 9 represents the optimized parameter combination obtained via response surface modeling. Unlike orthogonal experimental designs limited to discrete factor levels, RSM builds a continuous regression model across the design space, enabling the identification of optimal conditions beyond the original design points.

Notably, the optimal solution lies within the interior of the design cube but does not coincide with any simulated experiment, highlighting the model's strong interpolation and generalization capabilities. This confirms the effectiveness of RSM in capturing nonlinear, multi-factor interactions and identifying improved solutions in previously unexplored regions—an essential advantage for investment casting process optimization.

4 Conclusions

Based on RSM, a predictive model for dimensional deformation and process parameter optimization was developed for the investment casting of turbine blades. The effects of key parameters—including pouring temperature, shell temperature, and withdrawal rate—on the dimensional response were systematically investigated. The main conclusions are as follows:

1) Sensitivity analysis revealed that withdrawal rate is the dominant factor, while shell temperature exhibits a "U"-shaped nonlinear relationship with deformation. Significant interactions among parameters were observed, indicating the need for coordinated regulation to optimize forming quality.
2) The constructed second-order RSM model demonstrated strong fitting accuracy, with a coefficient of determination R^2= 0.978 and a RMSE of 0.0026. The model effectively captures the complex nonlinear relationships between process parameters and deformation response.
3) RSM enables the prediction of optimal parameter combinations beyond the originally tested design points. The optimized process reduced the predicted deformation from 0.2047 mm to 0.1905 mm, achieving a reduction of approximately 6.95%, thereby validating the adaptability and effectiveness of RSM in complex casting process optimization.

Acknowledgments

The authors greatly acknowledge the financial support from the Scientific and the National Science and Technology Major Project (Grant No. J2019-VII-0013-0153) and Innovation Capability Support Program of Shaanxi (No. 2022TD-60).

Conflicts of interest:

The authors declare that they have no known competing financial interests or personal relationships that could have appeared to influence the work reported in this paper.

References

[1] Reed R C. The superalloys fundamentals and applications. Cambridge: Cambridge University Press; 2008.
[2] Mathur H N, Panwisawas C, Jones C N, et al. Nucleation of recrystallisation in castings of single crystal ni-based superalloys. Acta Mater., 2017, 129: 112 – 123.
[3] Pollock T M. Alloy design for aircraft engines. Nat. Mater., 2016, 15: 809 – 815.

[4] Ren S, Bu K, Zhang R, et al. Effect of constraint removal on single-crystal blade dimensions during investment casting. J. Manuf. Process., 2024, 119: 73 – 86.

[5] Kermanpur A, M. M, N. V, et al. Improvement of grain structure and mechanical properties of a land based gas turbine blade directionally solidified with liquid metal cooling process. Mater. Sci. Technol., 2008, 24: 100 – 106.

[6] Xu Q, Zhang H, Liu B. Multiscale modelling and simulation of single crystal superalloy turbine blade casting during directional solidification process. China Foundry, 2014, 9 – 11.

[7] Singh R, Singh J. Investigating the effect of shape factor, slurry layers and pouring temperature in precision investment casting. Mater. Sci. Forum, 2013, 751: 35 – 44.

[8] Ren S, Bu K, Mou S, et al. Control of dimensional accuracy of hollow turbine blades during investment casting. J. Manuf. Process., 2023, 99: 548 – 562.

[9] Qian C, Kaminer I, Chen H. A guidance to intelligent metamaterials and metamaterials intelligence. Nat. Commun., 2025, 16: 1154.

[10] Pattnaik S, Karunakar D B, Jha P K. Developments in investment casting process—a review. J. Mater. Process. Technol., 2012, 212: 2332 – 2348.

[11] Wang F, Liu Y, Yang Q, et al. Microscale stray grains formation in single-crystal turbine blades of ni-based superalloys. J. Mater. Sci. Technol., 2024, 191: 134 – 145.

[12] Dini H, Andersson N-E, Jarfors A E W. Effect of process parameters on distortion and residual stress of high-pressure die-cast az91d components. Int J Metalcast, 2018, 12: 487 – 497.

[13] Ma D. Development of single crystal solidification technology for production of superalloy turbine blades. Acta Metall. Sin., 2015, 51: 1179 – 1190.

[14] Miller J D, Pollock T M. Process simulation for the directional solidification of a tri-crystal ring segment via the Bridgman and liquid-metal-cooling processes. Metall. Mater. Trans. A., 2012, 43: 2414 – 2425.

[15] Galantucci L M, Tricarico L. A computer-aided approach for the simulation of the directional-solidification process for gas turbine blades. J. Mater. Process. Technol., 1998, 77: 160 – 165.

[16] Tian J-W, Bu K, Song J-H, et al. Optimization of investment casting process parameters to reduce warpage of turbine blade platform in dd6 alloy. China Foundry, 2017, 14: 469 – 477.

[17] Niranjan K, Lakshminarayanan P R. Optimization of process parameters for in situ casting of al/tib2 composites through response surface methodology. Transactions of Nonferrous Metals Society of China, 2013, 23: 1269 – 1274.

[18] Szeliga D, Kubiak K, Sieniawski J. Control of liquidus isotherm shape during solidification of Ni-based superalloy of single crystal platforms. J. Mater. Process. Technol., 2016, 234: 18 – 26.

[19] Ma D, Bührig-Polaczek A. Application of a heat conductor technique in the production of single-crystal turbine blades. Metallurgical and Materials Transactions A, 2009, 40: 738 – 748.

[20] Aguilar J, Schievenbusch A, Kättlitz O. Investment casting technology for production of tial low pressure turbine blades – process engineering and parameter analysis. Intermetallics, 2011, 19: 757 – 761.

[21] Campbell J. Complete casting handbook (second edition). Boston: Butterworth-Heinemann; 2015.

[22] Zhang H, Liu X, Ma D, et al. Digital twin for directional solidification of a single-crystal turbine blade. Acta Mater., 2023, 244: 118579.

[23] Szeliga D, Kubiak K, Motyka M, et al. Directional solidification of Ni-based superalloy castings thermal analysis. Vacuum, 2016, 327 – 342.

[24] Gromada M, Świeca A, Kostecki M, et al. Ceramic cores for turbine blades via injection moulding. J. Mater. Process. Technol., 2015, 220: 107 – 112.

[25] Hallensleben P, Schaar H, Thome P, et al. On the evolution of cast microstructures during processing of single crystal Ni-base superalloys using a Bridgman seed technique. Mater Design, 2017, 128: 98 – 111.

[26] Khandelwal H, Ravi B. Effect of varying part geometry and mold constraints on dimensional deviations of sand cast parts. International Journal on Interactive Design and Manufacturing (IJIDeM), 2025, 19: 4973 – 4986.

[27] Szeliga D. Effect of processing parameters and shape of blade on the solidification of single-crystal cmsx-4 Ni-based superalloy. Metall Mater Trans B, 2018, 49: 2550 – 2570.

[28] Allaix D L, Carbone V I. An improvement of the response surface method. Structural Safety, 2011, 33: 165 – 172.

[29] Kumar A, Ramadas H, Kumar C S, et al. Laser polishing of additive manufactured stainless-steel parts by line focused beam: A response surface method for improving surface finish. J. Manuf. Process., 2025, 133: 1310 – 1328.

[30] Jadhav P, Krishnan S, Patil R, et al. Improving biogas production with application of trimetallic nanoparticle using response surface methods. Renewable Energy, 2024,

234: 121199.

[31] Tiwari S, Kumar A, Gupta N, et al. Hydrogen storage systems performance and design parameters using response surface methods and sensitivity analysis. Renewable and Sustainable Energy Reviews, 2024, 202: 114628.

[32] Lal B, Dey A. Fretting wear characteristics of ti6al4v/tic nano composites using response surface method. Tribology International, 2024, 193: 109412.

[33] Zheng P, Zhang H, Zhang Z, et al. Parameter optimization method of contra-rotating vertical axis wind turbine: Based on numerical simulation and response surface. Journal of Cleaner Production, 2024, 435: 140475.

[34] Rojas-López A G, Villarreal-Cervantes M G, Rodríguez-Molina A. Surrogate indirect adaptive controller tuning based on polynomial response surface method and bioinspired optimization: Application to the brushless direct current motor controller. Expert Systems with Applications, 2024, 245: 123070.